Concentration-dependent circularly polarized luminescence (CPL) of chiral *N*,*N*'-dipyrenyldiamines: sign-inverted CPL switching between monomer and excimer regions under retention of the monomer emission for photoluminescence

Suguru Ito,*[a] Kengo Ikeda,[a] Shoma Nakanishi,[b] Yoshitane Imai,*[b] and Masatoshi Asami*[a]

[a] *Department of Advanced Materials Chemistry, Graduate School of Engineering*
YOKOHAMA National University
79-5 Tokiwadai, Hodogaya-ku, Yokohama 240-8501, Japan
*E-mail: suguru-ito@ynu.ac.jp, m-asami@ynu.ac.jp

[b] *Department of Applied Chemistry, Faculty of Science and Engineering*
Kindai University
3-4-1 Kowakae, Higashi-Osaka, Osaka 577-8502, Japan
*E-mail: y-imai@apch.kindai.ac.jp

Table of contents

1. General

All air-sensitive experiments were carried out under an atmosphere of argon unless otherwise noted. IR spectra were recorded on a Nicolet iS10 FT-IR spectrometer. ^{1}H and ^{13}C NMR spectra were recorded on JEOL ECX-400 or Bruker DRX-500 spectrometer using tetramethylsilane or solvent residual signal as an internal standard. Optical rotations were measured on a JASCO P-1000 automatic polarimeter. HPLC analyses were carried out with JASCO instruments (pump, PU-2080 plus; detector, UV-2075). The enantiomeric excesses were determined by HPLC using Daicel Chiralcel OD-H (25 cm × 0.46 cm i.d.) column. Elemental analyses were carried out on a Vario EL III Elemental analyzer. High-resolution mass spectra (HRMS) were recorded on a JEOL JMS-600 mass spectrometer (EI) and a Hitachi Nano Frontier LD spectrometer (ESI). UV-vis absorption and photoluminescence (PL) spectra were measured on a JASCO V560 spectrophotometer and a JASCO FP-8300 fluorescence spectrometer, respectively. The absolute fluorescence quantum yields were determined using a 100 mmϕ integrating sphere JASCO ILF-835. Circular dichroism (CD) and circularly polarized luminescence (CPL) spectra were recorded on a JASCO J-725 and a JASCO CPL-300 spectrometer, respectively. The value of g_{CD} is experimentally defined as $\Delta\varepsilon/\varepsilon$ = [ellipticity/32,980] / absorbance at a CD wavelength, and the value of g_{em} is experimentally defined as $\Delta I/I$ = [ellipticity/(32,980/ln10)] / unpolarised PL intensity at a CPL wavelength. UV-vis absorption, CD, PL, and CPL spectra were measured in a quartz cell (light path 10 mm, 1 mm, or 0.1 mm). TLC analyses were done on silica-gel 60 F_{254}-precoated aluminum backed sheets (E. Merck). Silica gel 60 N (spherical, neutral, 63–210 μm) was used for column chromatography. A hexane solution of diethylzinc (1.1 M, Kanto Chemical Co., Inc., Japan) was used for the enantioselective addition. Tetrahydrofuran (dehydrated, stabilizer free) were purchased from Kanto Chemical Co., Inc. Other solvents were purified and dried according to standard procedures. The spectroscopic grade solvents for UV–vis absorption, PL, CD, and CPL measurements were purchased from Kanto Chemical Co., Inc. and Wako Pure Chemical Industries, Ltd. (*R*,*R*)- and (*S*,*S*)-4,6-bis(1-aminopropyl)dibenzo[*b*,*d*]furan (**S1**)[1] and (2-((3*R*,7a*S*)-2-phenylhexahydro-1*H*-pyrrolo[1,2-*c*]imidazol-3-yl)phenyl)bis(3-(trifluoromethyl)phenyl)methanol (**S2**)[2] were prepared by our previously reported procedure. Dibenzo[*b*,*d*]furan-4-carbaldehyde (**S3**) was synthesized according to the literature procedure.[3]

2. Synthesis of chiral fluorophores (*R*,*R*)-1, (*S*,*S*)-1, and (*R*)-2

*2.1. Synthesis of (R,R)-4,6-bis(1-(pyren-1-ylamino)propyl)dibenzo[b,d]furan (**1**)*

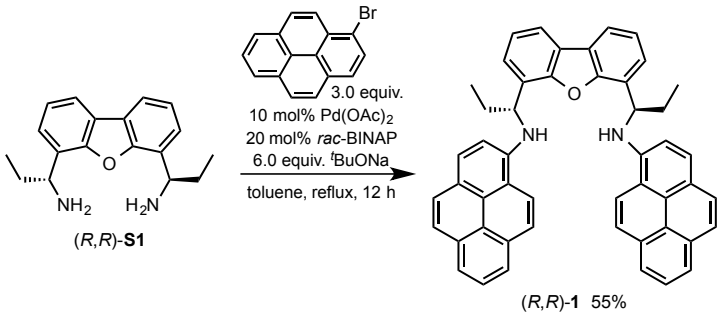

Scheme S1 Synthesis of (*R*,*R*)-4,6-bis(1-(pyren-1-ylamino)propyl)dibenzo[*b*,*d*]furan (**1**).

A mixture of ^{t}BuONa (180 mg, 1.9 mmol), *rac*-BINAP (39 mg, 63 μmol), and $Pd(OAc)_2$ (7 mg, 32 μmol) in degassed toluene (4.0 mL) was stirred at room temperature for 30 min. To the mixture was added a toluene (4.0 mL) solution of (*R*,*R*)-4,6-bis(1-aminopropyl)dibenzo[*b*,*d*]furan (**S1**) (89 mg, 0.32 mmol) and a toluene solution (4.0 mL) of 1-bromopyrene (270 mg, 0.95 mmol) consecutively and the mixture was refluxed for 12 h. The reaction mixture was diluted with dichloromethane and then filtered through Celite. After the filtrate was concentrated under reduced pressure, crude product was purified by silica-gel column chromatography (Silica gel 60N (15 g), hexane/dichloromethane =3:1 and Silica gel 60N (44 g), toluene/cyclohexane/dichloromethane=2:1:1) to give (*R*,*R*)-**1** (120 mg, 55%) as a yellow solid.

(*R*,*R*)-4,6-Bis(1-(pyren-1-ylamino)propyl)dibenzo[*b*,*d*]furan (1)

Yellow solid; M.p. 236.1–237.1 °C; $[\alpha]_D^{29}$ –1145.1 (*c* 0.25, DMSO); IR (KBr): ν_{max} 3433, 3032, 2955, 2920, 2873, 1602, 1520, 1487, 1431, 1412, 1332, 1303, 1284, 1236, 1183, 1136, 839, 829, 818, 783, 770, 746, 715 cm^{-1}; ^{1}H NMR (400MHz, d_6-DMSO): δ (ppm) 8.81 (d, *J* = 9.6 Hz, 2H), 8.03–7.95 (m, 6H), 7.88–7.82 (m, 4H), 7.71–7.60 (m, 6H), 7.53 (d, *J* = 8.5 Hz, 2H), 7.29–7.19 (m, 6H), 5.40 (br ddd, *J* = 9.6, 7.8, 7.3 Hz, 2H), 2.49 (ddq, *J* = 13.8, 7.8, 7.3 Hz, 2H), 2.31 (dqd, *J* = 13.8, 7.3, 6.3 Hz, 2H), 1.16 (t, *J* = 7.3 Hz, 6H); ^{13}C NMR (100 MHz, d_6-DMSO): δ (ppm) 153.6, 142.6, 132.0, 131.5, 128.2, 127.5, 126.3, 126.0, 125.7, 125.4, 125.0, 124.7, 123.6, 123.22, 123.16, 122.7, 122.3, 121.8, 121.3, 119.5, 115.9, 109.3, 54.6, 29.3, 11.6; ESI-HRMS (*m*/*z*): $[M+H]^+$ Calcd for $C_{50}H_{39}N_2O$, 683.3047; Found, 683.3057.

*2.2. Synthesis of (S,S)-4,6-bis(1-(pyren-1-ylamino)propyl)dibenzo[b,d]furan (**1**)*

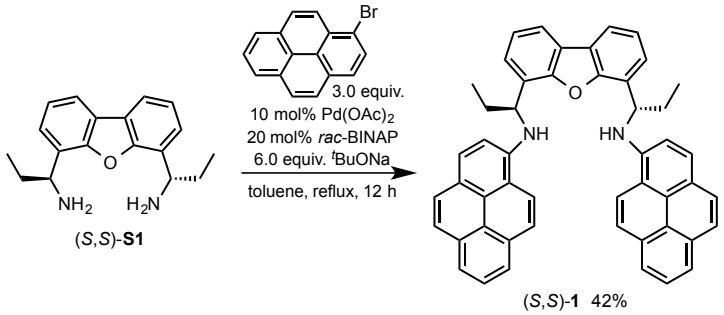

Scheme S2 Synthesis of (*S*,*S*)-4,6-bis(1-(pyren-1-ylamino)propyl)dibenzo[*b*,*d*]furan (**1**).

According to the same experimental procedure as the synthesis of (*R*,*R*)-**1**, the mixture of (*S*,*S*)-**S1** (87 mg, 0.31 mmol) and 1-bromopyrene (260 mg, 0.93 mmol) in the presence of ^{t}BuONa (180 mg, 1.9 mmol), *rac*-BINAP (39 mg, 62 μmol), and $Pd(OAc)_2$ (7 mg, 31 μmol) was refluxed in degassed toluene (8.0 mL) for 12 h to give (*S*,*S*)-**1** (89 mg, 42%) as a yellow solid.

(*S*,*S*)-4,6-Bis(1-(pyren-1-ylamino)propyl)dibenzo[*b*,*d*]furan (1)

Yellow solid; M.p. 236.3–237.3 °C; $[\alpha]_D^{29}$ +1245.0 (*c* 0.25, DMSO). IR and NMR spectra of (*S*,*S*)-**1** were in good agreement with those of (*R*,*R*)-**1**.

*2.3. Synthesis of (R)-4-(1-(pyren-1-ylamino)propyl)dibenzo[b,d]furan (**2**)*

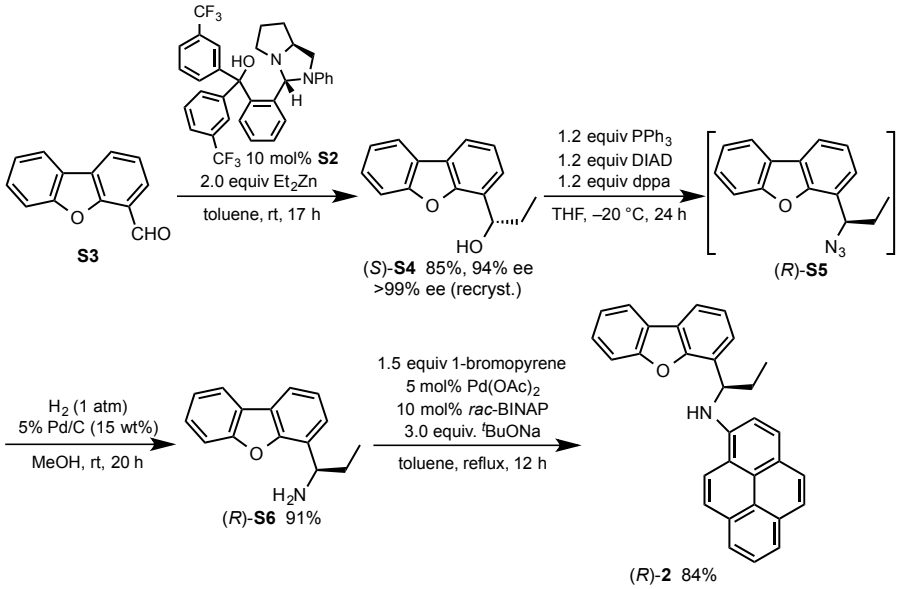

Scheme S3 Synthesis of (*R*)-4-(1-(pyren-1-ylamino)propyl)dibenzo[*b*,*d*]furan (**2**).

2.3.1. Synthesis of (*S*)-1-(dibenzo[*b*,*d*]furan-4-yl)propan-1-ol (**S4**)

To a stirred solution of 1,4-amino alcohol **S2** (0.36 g, 0.61 mmol) in toluene (30 mL), a hexane solution (1.1 M) of diethylzinc (12 mmol, 11 mL) was added dropwise through a syringe at 0 °C. The reaction mixture was stirred at room temperature for 30 min. To the mixture was added dropwise a toluene (30 mL) solution of dibenzo[*b*,*d*]furan-4-carbaldehyde (**S3**) (1.2 g, 6.1 mmol) and the mixture was stirred at room temperature for 17 h. Saturated aqueous ammonium chloride solution and 2M aqueous HCl were added to the reaction mixture. The aqueous layer was separated and the organic layer was extracted with CH_2Cl_2 three times. The combined organic layer was washed with water and brine, and dried over anhydrous Na_2SO_4. After removal of solvent under reduced pressure, crude product was purified by silica-gel column chromatography (Silica gel 60N (100 g), hexane/dichloromethane/ethyl acetate=2:1:1) to give (*S*)-**S4** (1.2 g, 85%, 94% ee) as a white solid. Enantiomerically pure (*S*)-**S4** (>99% ee) was obtained by a single recrystallization from hexane.

(*S*)-1-(Dibenzo[*b*,*d*]furan-4-yl)propan-1-ol (S4)

White solid; M.p. 83.2–84.3 °C; $[\alpha]_D^{19}$ –33.1 (*c* 1.0, $CHCl_3$); IR (KBr): ν_{max} 3355, 3286, 3058, 2967, 2956, 2927, 2868, 2466, 1453, 1421, 1267, 1185, 1125, 1101, 1043, 976, 845, 750 cm^{-1}; ^1H NMR (400MHz, $CDCl_3$): δ (ppm) 7.94 (d, *J* = 7.5 Hz, 1H), 7.85 (dd, *J* = 7.8, 1.4 Hz, 1H), 7.58 (d, *J* = 8.0 Hz, 1H), 7.49–7.43 (m, 2H), 7.36–7.31 (m, 2H), 5.19 (br td, *J* = 6.5, 4.8 Hz, 1H), 2.28 (br d, *J* = 4.8 Hz, 1H), 2.03 (qd, *J* = 7.4, 6.5 Hz, 2H), 1.00 (t, *J* = 7.4 Hz, 3H); ^{13}C NMR (100 MHz, $CDCl_3$): δ (ppm) 156.0, 153.1, 128.6, 127.1, 124.3, 124.2, 124.1, 122.8, 122.7, 120.6, 119.5, 111.7, 71.7, 30.6, 10.2; EI-HRMS (*m*/*z*): $[M]^+$ Calcd for $C_{15}H_{14}O_2$, 226.0994; Found, 226.0985.

(*S*)-Configuration of **S4** should be constructed based on the stereochemical course of the reaction reported previously.[2] The enantiomeric excess of (*S*)-**S4** after recrystallization was determined to be >99% as the minor isomer (*R*)-**S4** was not detected by HPLC analysis using a chiral column (Daicel Chiralcel OD-H; 254 nm UV detector; eluent hexane/*i*-PrOH=90:10; flow rate 0.5 mL/min; *t*, 15.2 min for (*R*)-**S4**, 19.5 min for (*S*)-**S4**). The retention time of (*R*)-**S4** was determined by using *rac*-**S4** prepared by the reaction of ethylmagnesium bromide with **S3**.

2.3.2. Synthesis of (*R*)-1-(dibenzo[*b*,*d*]furan-4-yl)propan-1-amine (**S6**)

To a stirred solution of (*S*)-**S4** (0.30 g, 1.3 mmol) and triphenylphosphine (0.41 g, 1.6 mmol) in THF (12 mL), a toluene solution (ca. 1.9 M) of diisopropyl azodicarboxylate (DIAD: 0.82 mL, 1.6 mmol) was added dropwise through a syringe at –20 °C. After the reaction mixture was stirred at –20 °C for 10 min, diphenylphosphoryl azide (dppa: 0.34 mL, 1.6 mmol) was added dropwise to the mixture through a syringe. The reaction mixture was stirred at –20 °C for 24 h, and then the solvent was removed under reduced pressure. After crude product was purified by silica-gel column chromatography (Silica gel 60N (80 g), hexane/dichloromethane/ethyl acetate=5:1:1), almost pure azide (*R*)-4-(1-azidopropyl)dibenzo[*b*,*d*]furan (**S5**) (0.30 g) was obtained as a colorless oil and used directly in the next step.

To a stirred solution of (*R*)-**S5** (0.30 g) in MeOH (10 mL) was added 5% Pd/C (46 mg, 15 wt%) and the mixture was stirred under H_2 atmosphere (1 atm balloon) at room temperature for 20 h. The reaction mixture was filtered through Celite to remove Pd/C. After the filtrate was concentrated under reduced pressure, (*R*)-**S6** (0.27 g, 91%) was obtained as a white solid.

(*R*)-1-(Dibenzo[*b*,*d*]furan-4-yl)propan-1-amine (S6)

White solid; M.p. 57.4–58.6 °C; $[\alpha]_D^{19}$ +13.1 (*c* 1.0, $CHCl_3$); IR (KBr): ν_{max} 3347, 3250, 3173, 3059, 2962, 2926, 2915, 2871, 1451, 1420, 1267, 1185, 935, 884, 845, 796, 756 cm^{-1}; ^1H NMR (400MHz, $CDCl_3$): δ (ppm) 7.94 (d, *J* = 7.3 Hz, 1H), 7.83 (dd, *J* = 7.6, 1.2 Hz, 1H), 7.59 (d, *J* = 8.2 Hz, 1H), 7.48–7.37 (m, 2H), 7.36–7.28 (m, 2H), 4.34 (t, *J* = 7.0 Hz, 1H), 1.99 (dqd, *J* = 13.0, 7.4, 7.0 Hz, 1H), 1.92 (dqd, *J* = 13.0, 7.4, 7.0 Hz, 1H), 0.94 (t, *J* = 7.4 Hz, 3H); ^{13}C NMR (100 MHz, $CDCl_3$): δ (ppm) 155.9, 153.7, 130.6, 127.0, 124.6, 124.3, 124.2, 122.8, 122.6, 120.6, 118.9, 111.7, 53.6, 30.8, 11.1; Anal. Calcd for $C_{15}H_{15}NO$: C, 79.97; H, 6.71; N, 6.22. Found: C, 79.86; H, 6.66; N, 6.09.

2.3.3. Synthesis of (*R*)-4-(1-(pyren-1-ylamino)propyl)dibenzo[*b*,*d*]furan (**2**)

According to the same experimental procedure as the synthesis of (*R*,*R*)-**1**, the mixture of (*R*)-**S6** (100 mg, 0.44 mmol) and 1-bromopyrene (190 mg, 0.66 mmol) in the presence of ^{t}BuONa (130 mg, 1.3 mmol), *rac*-BINAP (27 mg, 44 μmol), and $Pd(OAc)_2$ (5 mg, 22 μmol) was refluxed in degassed toluene (9.0 mL) for 12 h. Crude product was purified by silica-gel column chromatography (Silica gel 60N (25 g), hexane/dichloromethane =3:1) to give (*R*)-**2** (160 mg, 84%) as a yellow solid.

(*R*)-4-(1-(Pyren-1-ylamino)propyl)dibenzo[*b*,*d*]furan (2)

Yellow solid; M.p. 87.0–88.0 °C; $[\alpha]_D^{21}$ –943.0 (*c* 0.25, DMSO); IR (KBr): ν_{max} 3434, 3037, 2962, 2929, 2872, 1602, 1518, 1487, 1450, 1423, 1282, 1184, 839, 830, 752, 712 cm^{-1}; ^1H NMR (400MHz,

d_6-DMSO): δ (ppm) 8.73 (d, J = 9.4 Hz, 1H), 8.14–8.10 (m, 1H), 8.09–8.04 (m, 2H), 8.00–7.97 (m, 1H), 7.95 (dd, J = 7.7, 1.3 Hz, 1H), 7.89 (t, J = 7.7 Hz, 1H), 7.85 (d, J = 8.2 Hz, 1H), 7.81 (d, J = 8.5 Hz, 1H), 7.74 (d, J = 8.9 Hz, 1H), 7.67 (d, J = 8.9 Hz, 1H), 7.61 (dd, J = 7.1, 1.3 Hz, 1H), 7.59–7.53 (m, 1H), 7.41 (td, J = 7.6, 0.9 Hz, 1H), 7.27 (t, J = 7.7 Hz, 1H), 7.15-7.10 (m, 2H), 5.31 (ddd, J = 9.3, 7.8, 6.3 Hz, 1H), 2.32 (ddq, J = 13.7, 7.8, 7.3 Hz, 1H), 2.16 (dqd, J = 13.7, 7.3, 6.3 Hz, 1H), 1.13 (t, J = 7.3 Hz, 3H); ^{13}C NMR (100 MHz, d_6-DMSO): δ (ppm) 155.5, 153.6, 142.6, 132.0, 131.5, 128.3, 127.62, 127.58, 126.5, 126.0, 125.4, 125.0, 124.7, 124.5, 123.8, 123.40, 123.36, 123.2, 122.7, 122.4, 121.7, 121.5, 121.2, 119.5, 116.1, 111.9, 109.2, 53.7, 29.5, 11.7 (one signal is hidden due to the incidental overlapping); ESI-HRMS (m/z): $[M+H]^+$ Calcd for $C_{31}H_{24}NO$, 426.1852; Found, 426.1852.

3. Supplementary spectral data

*3.1. PL spectra of (R,R)-**1** and (R)-**2** in diluted solution*

The maximum PL wavelength of 1.0×10^{-5} M toluene solution of (*R*,*R*)-**1** was in good agreement with those of 1.0×10^{-6} M toluene solution of (*R*,*R*)-**1** and 1.0×10^{-5} M toluene solution of (*R*)-**2**, indicating that this PL band should be assigned to the monomer emission of (*R*,*R*)-**1** (Fig. S1).

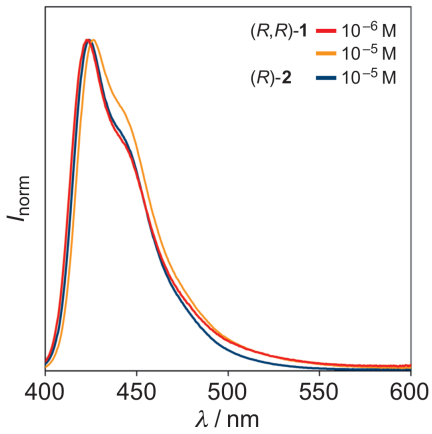

Fig. S1 PL spectra of (*R*,*R*)-**1** in toluene (1.0×10^{-6} and 1.0×10^{-5} M) and (*R*)-**2** in toluene (1.0×10^{-5} M).

*3.2. Unnormalized PL spectra of (R,R)-**1** in different concentrations*

The intensity of PL band for 1.0×10^{-4} M toluene solution was larger than that of 1.0×10^{-5} M solution as the amount of absorbed photons increased for the 1.0×10^{-4} M solution. The amount of absorbed photons were saturated for 1.0×10^{-3} M and saturated solutions, and the intensity of their PL bands decreased compared with the 1.0×10^{-4} M solution on account of the self-absorption of the luminescence (Fig. S2).

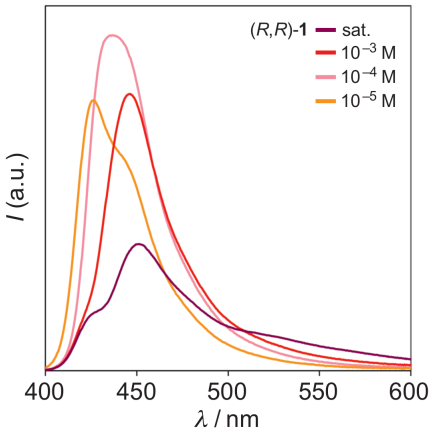

Fig. S2 Unnormalized PL spectra of (*R*,*R*)-**1** in toluene [1.0×10^{-5} M, 1.0×10^{-4} M, 1.0×10^{-3} M, and 8.0×10^{-3} M (saturated solution)].

*3.3. Determination of the concentration for the saturated toluene solution of (R,R)-**1***

The concentration of the saturated toluene solution of (*R*,*R*)-**1** was determined by ^{1}H NMR analysis using 1,3,5-trimethoxybenzene (**S7**) as an internal standard. A saturated d_8-toluene solution of (*R*,*R*)-**1** (solution A) was prepared by filtering a suspension of (*R*,*R*)-**1** (5.5 mg, 8.0 $\times 10^{-3}$ mmol) in d_8-toluene (0.80 mL) via a nylon membrane syringe filter (pore size: 0.22 μm). A 0.3 M d_8-toluene solution of **S7** (solution B) was prepared by dissolving **S7** (10.1 mg, 6.0 $\times 10^{-2}$ mmol) in d_8-toluene (0.20 mL). Solution A (590 μL) and solution B (10 μL) were mixed, and the ^{1}H NMR spectrum of the mixture was recorded. Based on the integral ratio of (*R*,*R*)-**1** and 1,3,5-trimethoxybenzene, the concentration of the saturated toluene solution of (*R*,*R*)-**1** was determined as 8.0×10^{-3} M (Fig. S3).

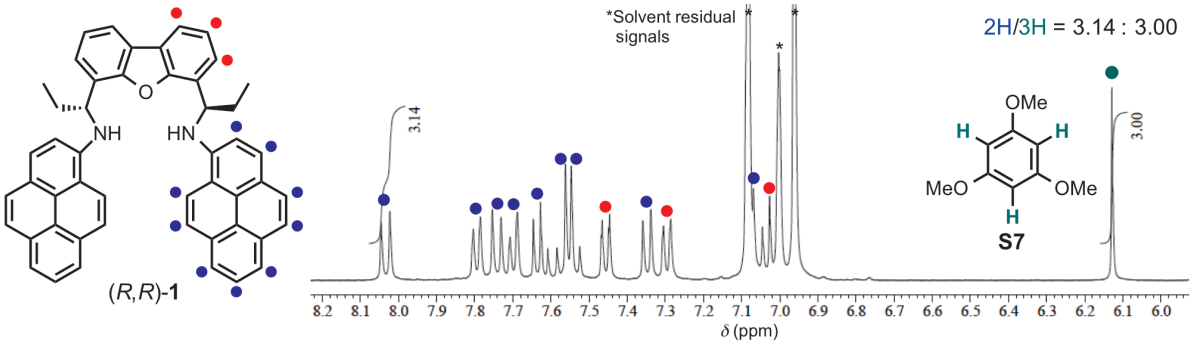

Fig. S3 Partial ^{1}H NMR spectrum of a saturated d_8-toluene solution of (*R*,*R*)-**1** in the presence of 1,3,5-trimethoxybenzene.

*3.4. CPL and PL spectra of (R,R)- and (S,S)-**1** in THF*

The switching of CPL band by increasing the concentration of **1** was also observed in THF (Fig. S4), although the efficiency for the excimer formation should be higher in toluene than in THF.

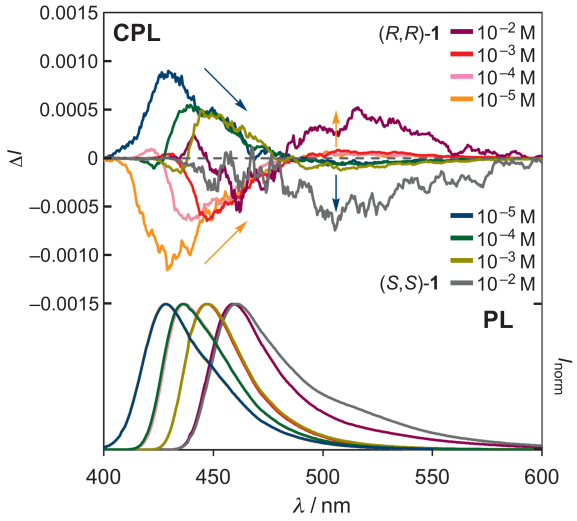

Fig. S4 CPL (top) and normalized PL (bottom) spectra of (*R*,*R*)-**1** (orange, pink, red, and purple lines) and (*S*,*S*)-**1** (blue, green, brown, and gray lines) in THF (1.0×10^{-5} M, 1.0×10^{-4} M, 1.0×10^{-3} M, and 1.0×10^{-2} M solution).

*3.5. Concentration-dependence of CPL and PL spectra for (R,R)-**S8** and (R)-**S9** in toluene*

The PL and CPL bands of (*R*,*R*)-**S8**[1] in toluene were observed in the same region regardless of the concentration (Fig. S5).

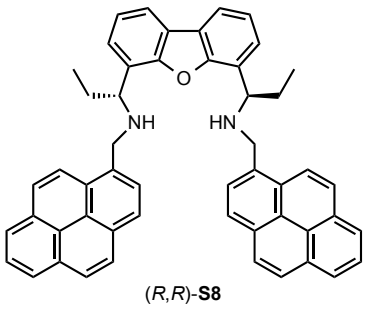

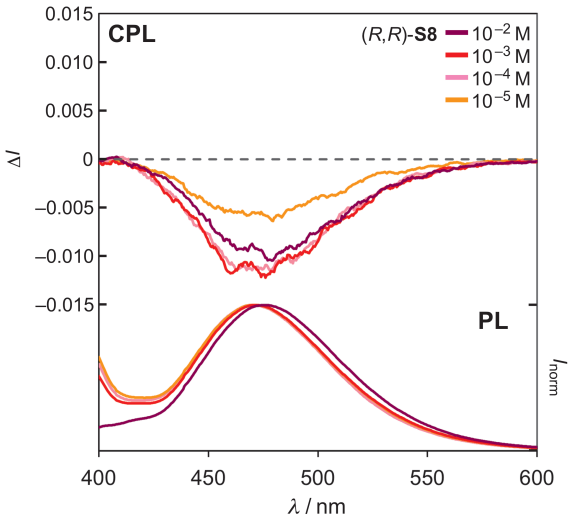

Fig. S5 CPL (top) and normalized PL (bottom) spectra of (*R*,*R*)-**S8** (orange, pink, red, and purple lines) in toluene (1.0×10^{-5} M, 1.0×10^{-4} M, 1.0×10^{-3} M, and 1.0×10^{-2} M solution).

The PL and CPL bands of (*R*)-**S9**[4] in toluene were also observed in the same region regardless of the concentration (Fig. S6).

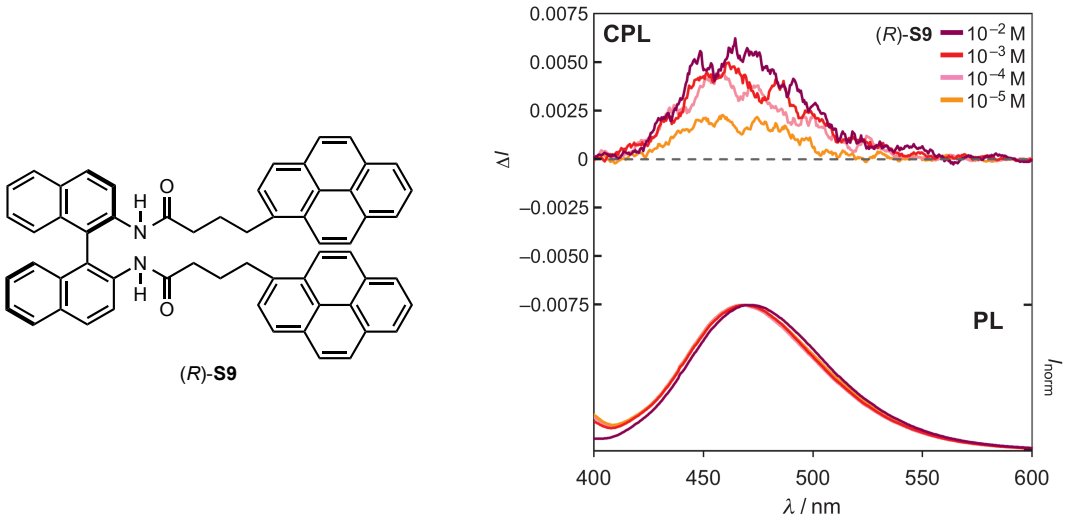

Fig. S6 CPL (top) and normalized PL (bottom) spectra of (*R*,*R*)-**S9** (orange, pink, red, and purple lines) in toluene (1.0×10^{-5} M, 1.0×10^{-4} M, 1.0×10^{-3} M, and 1.0×10^{-2} M solution).

*3.6. ^{1}H NMR spectra for concentrated solutions of (R,R)-**1***

No significant change has been observed in ^{1}H NMR spectra of (*R*,*R*)-**1** in d_8-toluene with different concentrations (Fig. S7).

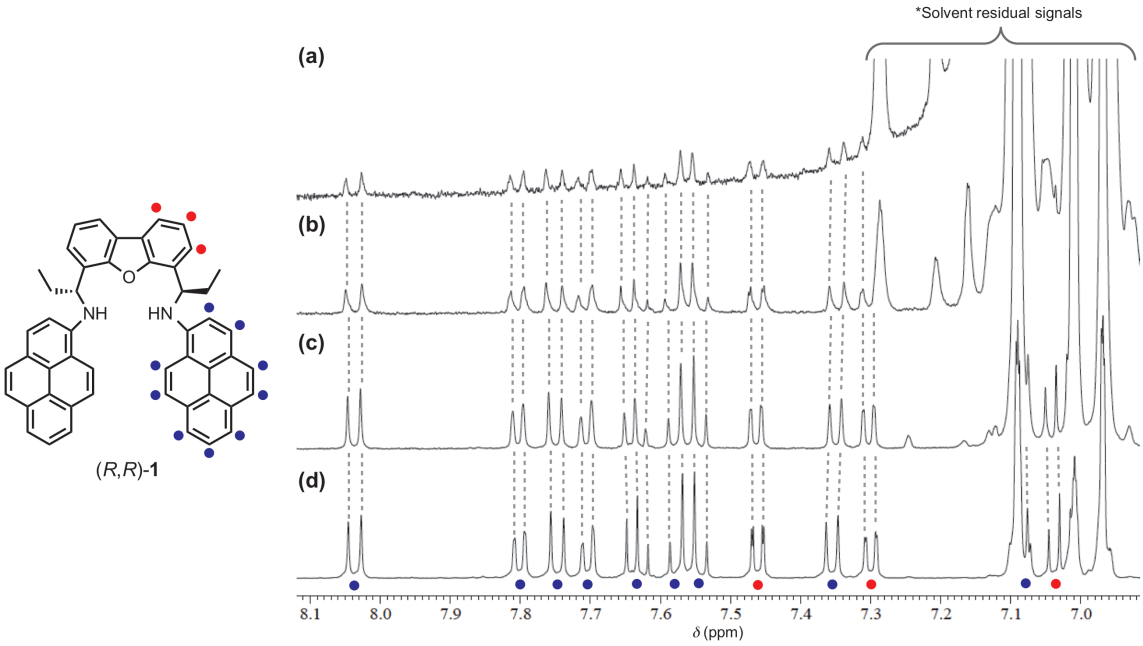

Fig. S7 Partially magnified ^{1}H NMR spectra of (*R*,*R*)-**1** in d_8-toluene (a) 1.0×10^{-5} M, 4096 scans (b) 1.0×10^{-4} M, 1024 scans (c) 1.0×10^{-3} M, 64 scans (d) 8.0×10^{-3} M, 8 scans.

*3.7. Spectral data for (R)-**2***

For mono-pyrenyl derivative (*R*)-**2**, the maximum CPL intensity was observed in the monomer region even for the highly concentrated toluene solution (1.0×10^{-2} M, Fig. S8), although a weak CPL band was observed in the excimer region.

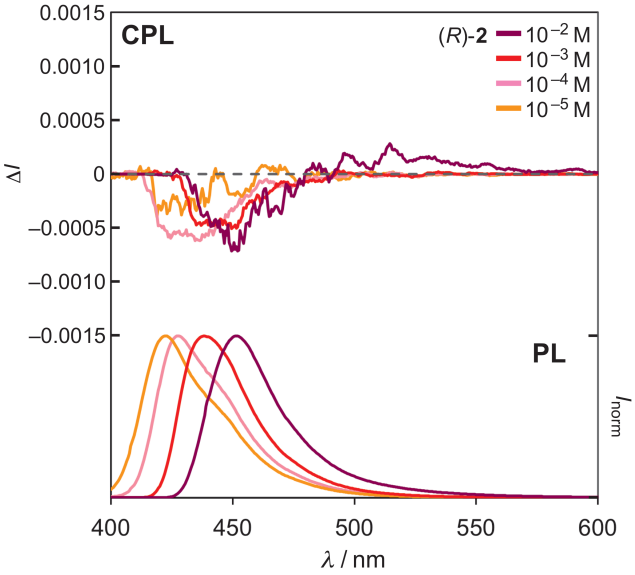

Fig. S8 CPL (top) and normalized PL (bottom) spectra of (*R*)-**2** (orange, pink, red, and purple lines) in toluene (1.0×10^{-5} M, 1.0×10^{-4} M, 1.0×10^{-3} M, and 1.0×10^{-2} M solution).

The CD and UV-vis absorption spectra of (*R*)-**2** were in good agreement with those of (*R*,*R*)-**1** with almost half intensities (Fig. S9).

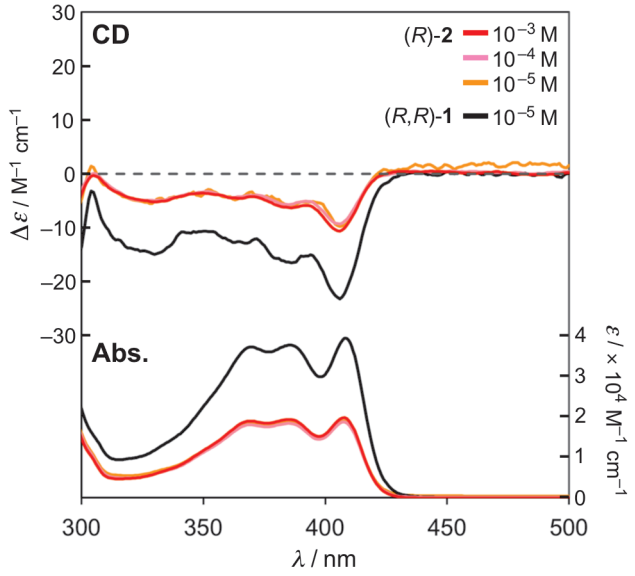

Fig. S9 CD (top) and absorption (bottom) spectra of (*R*)-**2** (orange, pink, and red lines) in toluene (1.0×10^{-5} M, 1.0×10^{-4} M, and 1.0×10^{-3} M) and (*R*,*R*)-**1** (black line) in toluene (1.0×10^{-5} M).

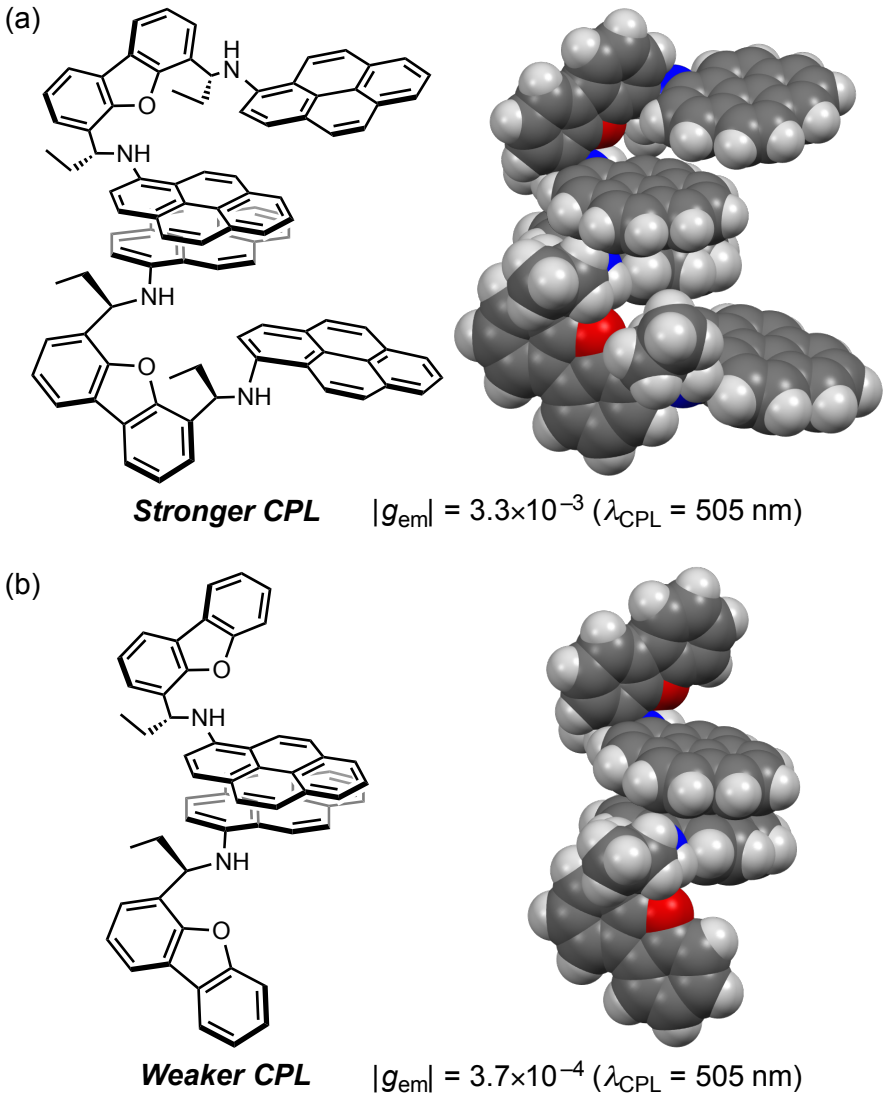

Fig. S10 Proposed structures for intermolecularly stacked (*R*,*R*)-**1** (a) and (*R*)-**2** (b).

4. Single-crystal X-ray diffraction analyses

*X-ray analysis of (R,R)-**1***

A single crystal of (*R*,*R*)-**1** was obtained from vapor diffusion of hexane into a diethyl ether solution of (*R*,*R*)-**1** and was mounted on a glass fiber. All measurements were made on a Rigaku Mercury70 diffractometer using graphite monochromated Mo-Kα radiation (λ = 0.71075 Å). The data were collected at a temperature of –50 ± 1 °C to a maximum 2θ value of 61.3°. A total of 744 oscillation images were collected. The crystal-to-detector distance was 45.00 mm. Readout was performed in the 0.137 mm pixel mode.

Of the 28146 reflections that were collected, 8084 were unique (R_{int} = 0.0833); equivalent reflections were merged. Data were collected and processed using CrystalClear(Rigaku).[5] The linear absorption coefficient, μ, for Mo-Kα radiation is 0.757 cm^{-1}. The data were corrected for Lorentz and polarization effects.

The structure was solved by direct methods (SIR2011)[6] and expanded using Fourier techniques. The non-hydrogen atoms were refined anisotropically. Hydrogen atoms were refined using the riding model. All calculations were performed using the CrystalStructure[7] crystallographic software package except for refinement, which was performed using SHELXL Version 2014/7.[8]

Crystal data for (*R*,*R*)-**1** (CCDC number 1531048): $C_{50}H_{38}N_2O$, M = 682.86, orthorhombic, a = 10.110(5) Å, b = 11.948(5) Å, c = 29.299(14) Å, V = 3539(3) Å^3, space group $P2_12_12_1$ (no. 19), Z = 4, D_c = 1.281 g cm^{-3}, F(000) = 1440.00, T = 223(1) K, μ(Mo-Kα) = 0.757 cm^{-1}, 28146 reflections measured, 8084 independent (R_{int} = 0.0833). The final refinement converged to R_1 = 0.0834 for $I > 2.0\sigma(I)$, wR_2 = 0.1639 for all data.

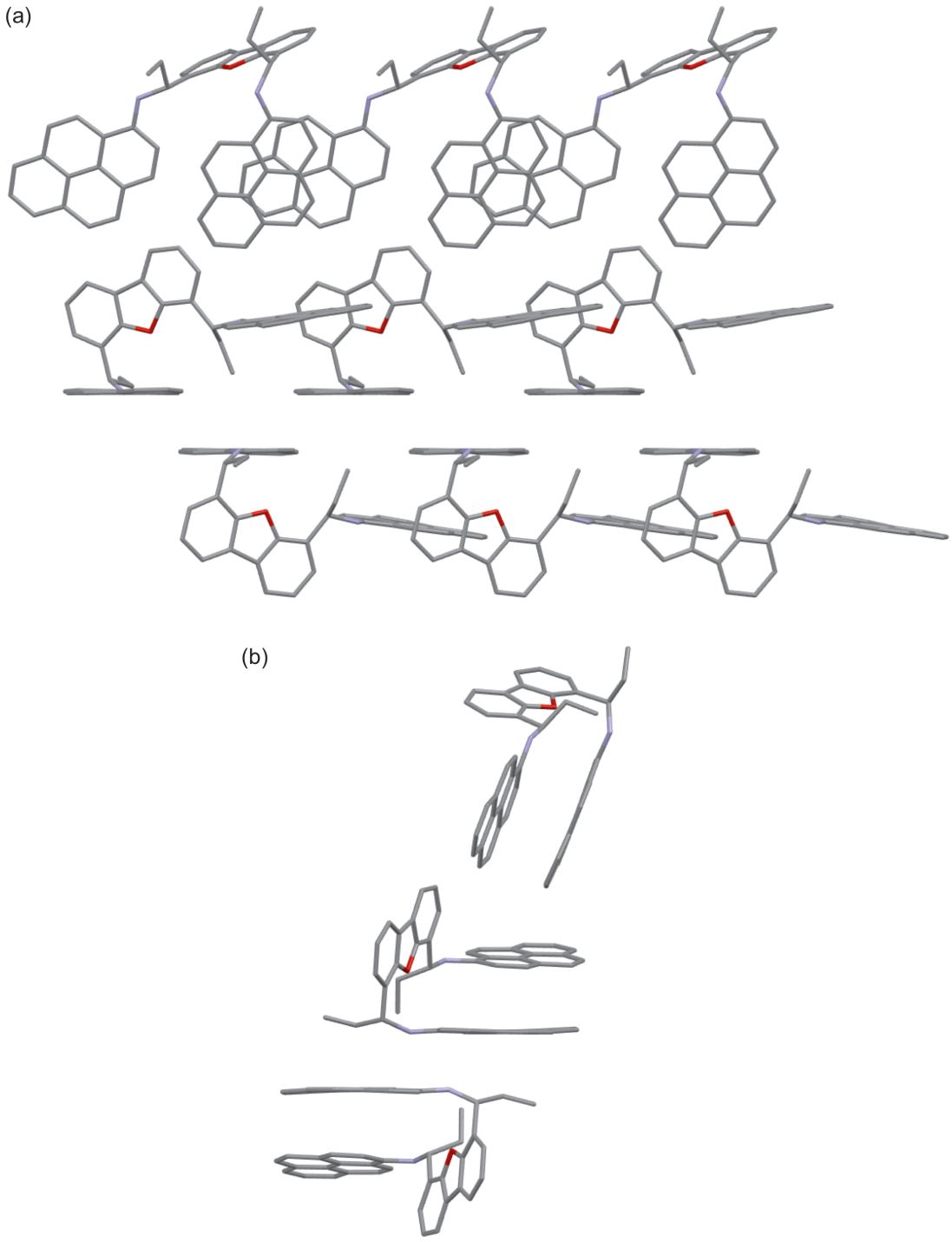

Fig. S11 (a) Front view and (b) side view of the packing structure of (*R*,*R*)-**1**. All hydrogen atoms were omitted for clarity. Color code: gray = C, red = O, blue = N.

*X-ray analysis of (S,S)-**1***

A single crystal of (*S*,*S*)-**1** was obtained from vapor diffusion of hexane into a diethyl ether solution of (*S*,*S*)-**1** and was mounted on a glass fiber. All measurements were made on a Rigaku Mercury70 diffractometer using graphite monochromated Mo-Kα radiation (λ = 0.71075 Å). The data were collected at a temperature of –50 ± 1 °C to a maximum 2θ value of 61.3°. A total of 744 oscillation images were collected. The crystal-to-detector distance was 45.00 mm. Readout was performed in the 0.137 mm pixel mode.

Of the 28325 reflections that were collected, 8126 were unique (R_{int} = 0.1129); equivalent reflections were merged. Data were collected and processed using CrystalClear(Rigaku).[5] The linear absorption coefficient, μ, for Mo-Kα radiation is 0.755 cm^{-1}. The data were corrected for Lorentz and polarization effects.

The structure was solved by direct methods (SIR2011)[6] and expanded using Fourier techniques. The non-hydrogen atoms were refined anisotropically. Hydrogen atoms were refined using the riding model. All calculations were performed using the CrystalStructure[7] crystallographic software package except for refinement, which was performed using SHELXL Version 2014/7.[8]

Crystal data for (*S*,*S*)-**1** (CCDC number 1531049): $C_{50}H_{38}N_2O$, M = 682.86, orthorhombic, a = 10.136(3) Å, b = 11.918(4) Å, c = 29.359(8) Å, V = 3546.4(18) Å^3, space group $P2_12_12_1$ (no. 19), Z = 4, D_c = 1.279 g cm^{-3}, F(000) = 1440.00, T = 223(1) K, μ(Mo-Kα) = 0.755 cm^{-1}, 28325 reflections measured, 8126 independent (R_{int} = 0.1129). The final refinement converged to R_1 = 0.1004 for $I > 2.0\sigma(I)$, wR_2 = 0.2128 for all data.

5. Theoretical calculations

The theoretical calculations were performed using Gaussian 09 program.[9] Molecular geometry of (*R*,*R*)-**1** was optimized using density functional theory (DFT) calculations at the B3LYP/6-31G(d) level of theory. The single-crystal X-ray structure of (*R*,*R*)-**1** (Fig. S12a,b) was used as a starting point. The optimized molecular structure of (*R*,*R*)-**1** exhibited almost no intramolecular stacks of two pyrene rings, indicating the structural difficulty for the formation of a stacked structure (Fig. S12c,d).

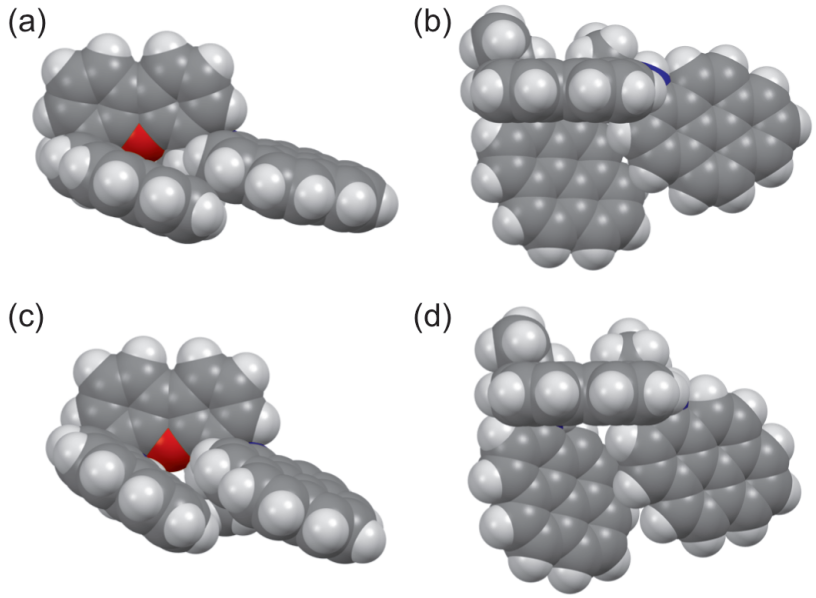

Fig. S12 Space filling models for (a) front view and (b) top view of X-ray structure of (*R*,*R*)-**1** and (c) front view and (d) top view of optimized molecular structure of (*R*,*R*)-**1** by DFT calculations at the B3LYP/6-31G(d) level of theory.

Table S1 Cartesian coordinates of optimized ground state geometries of (*R*,*R*)-**1**

(*R*,*R*)-**1** (B3LYP/6-31G(d) level)

E (au, no ZPE) = –2113.05671079

E (au, ZPE) = –2112.311969

Number of imaginary frequency: 0

Center Number	Atomic Number	Atomic Type	Coordinates (Angstroms) X	Y	Z
1	8	0	-2.505265	-2.080853	0.056764
2	7	0	1.769750	-2.816377	0.403705
3	1	0	2.273746	-3.384137	1.068541
4	7	0	-3.587615	0.268081	1.660078
5	1	0	-2.702845	-0.222212	1.672038
6	6	0	-1.747393	-2.742544	-0.894704
7	6	0	-0.413779	-3.111259	-0.725600
8	6	0	0.166519	-3.766442	-1.816644
9	1	0	1.209273	-4.057313	-1.740015
10	6	0	-0.552333	-4.035793	-2.992137
11	1	0	-0.052834	-4.544161	-3.811905
12	6	0	-1.887064	-3.661015	-3.125645
13	1	0	-2.436962	-3.872606	-4.038129
14	6	0	-2.497664	-2.999176	-2.054526
15	6	0	-3.819380	-2.455144	-1.795650
16	6	0	-5.019235	-2.380881	-2.512883
17	1	0	-5.097082	-2.794084	-3.514313
18	6	0	-6.109932	-1.761719	-1.909018
19	1	0	-7.052610	-1.689227	-2.443742
20	6	0	-6.009838	-1.216567	-0.618540
21	1	0	-6.879843	-0.731884	-0.181320
22	6	0	-4.827478	-1.268583	0.128900
23	6	0	-3.759679	-1.907651	-0.502957
24	6	0	0.322656	-2.863768	0.587625
25	1	0	-0.031384	-1.906691	1.002334

26	6	0	-0.031650	-3.965687	1.613161
27	1	0	-1.120719	-4.081867	1.612886
28	1	0	0.378998	-4.919023	1.252913
29	6	0	0.444247	-3.678166	3.042228
30	1	0	0.134508	-4.481933	3.718827
31	1	0	1.534784	-3.593613	3.117151
32	1	0	0.017786	-2.740735	3.418485
33	6	0	2.446449	-1.655937	0.027071
34	6	0	1.754614	-0.538754	-0.470426
35	1	0	0.678433	-0.575924	-0.589832
36	6	0	2.424979	0.629107	-0.812719
37	1	0	1.854708	1.478977	-1.178179
38	6	0	3.814475	0.744578	-0.675589
39	6	0	4.520386	1.953063	-0.991107
40	1	0	3.943615	2.805910	-1.341812
41	6	0	5.871961	2.041356	-0.852143
42	1	0	6.394134	2.964370	-1.092129
43	6	0	6.643426	0.920352	-0.389812
44	6	0	8.038453	0.983373	-0.241526
45	1	0	8.552602	1.910688	-0.482817
46	6	0	8.762973	-0.120820	0.205387
47	1	0	9.842311	-0.049573	0.311801
48	6	0	8.115110	-1.313930	0.514102
49	1	0	8.684691	-2.173668	0.858811
50	6	0	6.720074	-1.424823	0.383719
51	6	0	6.016462	-2.639010	0.675608
52	1	0	6.590294	-3.507657	0.989768
53	6	0	4.661243	-2.722474	0.551877
54	1	0	4.185460	-3.680264	0.743335
55	6	0	3.868194	-1.602494	0.127755
56	6	0	4.545496	-0.389692	-0.205764
57	6	0	5.966346	-0.299389	-0.070121
58	6	0	-4.710411	-0.663437	1.525159
59	1	0	-5.630914	-0.103340	1.724945

60	6	0	-4.580922	-1.734436	2.630694
61	1	0	-3.667673	-2.318133	2.456025
62	1	0	-4.441422	-1.202865	3.579556
63	6	0	-5.784147	-2.676147	2.728293
64	1	0	-5.645793	-3.393264	3.544630
65	1	0	-6.708415	-2.120510	2.929446
66	1	0	-5.930487	-3.244645	1.803964
67	6	0	-3.527531	1.499635	1.007968
68	6	0	-4.664239	2.085370	0.424028
69	1	0	-5.611939	1.561319	0.442600
70	6	0	-4.598873	3.320227	-0.207422
71	1	0	-5.499267	3.736428	-0.653522
72	6	0	-3.396321	4.031479	-0.308367
73	6	0	-3.299633	5.290383	-0.988259
74	1	0	-4.201888	5.703926	-1.433547
75	6	0	-2.116020	5.956112	-1.085048
76	1	0	-2.056804	6.907791	-1.607496
77	6	0	-0.917211	5.421027	-0.500698
78	6	0	0.317479	6.084290	-0.589452
79	1	0	0.368892	7.033315	-1.117884
80	6	0	1.465474	5.543394	-0.011876
81	1	0	2.410318	6.074738	-0.092226
82	6	0	1.410211	4.331099	0.671554
83	1	0	2.306913	3.914282	1.123402
84	6	0	0.195963	3.631235	0.787698
85	6	0	0.091963	2.390935	1.498711
86	1	0	0.982622	1.990447	1.975314
87	6	0	-1.091831	1.720062	1.585958
88	1	0	-1.122720	0.806937	2.172975
89	6	0	-2.291140	2.211730	0.967010
90	6	0	-2.226996	3.466811	0.287493
91	6	0	-0.985334	4.170970	0.193051

---

6. References

1) S. Ito, K. Ikeda and M. Asami, *Chem. Lett.*, 2016, **45**, 1379.

2) M. Asami, A. Hasome, N. Yachi, N. Hosoda, Y. Yamaguchi and S. Ito, *Tetrahedron: Asymmetry*, 2016, **27**, 322.

3) N. Lakshminarayana, Y. R. Prasad, L. Gharat, A. Thomas, S. Narayanan, A. Raghuram, C. V. Srinivasan and B. Gopalan, *Eur. J. Med. Chem.*, 2010, **45**, 3709.

4) K. Nakabayashi, S. Kitamura, N. Suzuki, S. Guo, M. Fujiki, Y. Imai, *Eur. J. Org. Chem.*, 2016, 64.

5) CrystalClear: Rigaku Corporation, 1999. CrystalClear Software User's Guide, Molecular Structure Corporation, (c) 2000. J. W. Pflugrath, *Acta Cryst*., 1999, **D55**, 1718.

6) SIR2011: M. C. Burla, R. Caliandro, M. Camalli, B. Carrozzini, G. L. Cascarano, C. Giacovazzo, M. Mallamo, A. Mazzone, G. Polidori and R. Spagna, *J. Appl. Cryst.*, 2012, **45**, 357.

7) Crystal Structure Analysis Package, Rigaku Corporation (2000-2014). Tokyo 196-8666, Japan.

8) G. M. Sheldrick, *Acta Cryst.*, 2008, **A64**, 112.

9) M. J. Frisch, G. W. Trucks, H. B. Schlegel, G. E. Scuseria, M. A. Robb, J. R. Cheeseman, G. Scalmani, V. Barone, B. Mennucci, G. A. Petersson, H. Nakatsuji, M. Caricato, X. Li, H. P. Hratchian, A. F. Izmaylov, J. Bloino, G. Zheng, J. L. Sonnenberg, M. Hada, M. Ehara, K. Toyota, R. Fukuda, J. Hasegawa, M. Ishida, T. Nakajima, Y. Honda, O. Kitao, H. Nakai, T. Vreven, J. A. Montgomery, Jr., J. E. Peralta, F. Ogliaro, M. Bearpark, J. J. Heyd, E. Brothers, K. N. Kudin, V. N. Staroverov, R. Kobayashi, J. Normand, K. Raghavachari, A. Rendell, J. C. Burant, S. S. Iyengar, J. Tomasi, M. Cossi, N. Rega, J. M. Millam, M. Klene, J. E. Knox, J. B. Cross, V. Bakken, C. Adamo, J. Jaramillo, R. Gomperts, R. E. Stratmann, O. Yazyev, A. J. Austin, R. Cammi, C. Pomelli, J. W. Ochterski, R. L. Martin, K. Morokuma, V. G. Zakrzewski, G. A. Voth, P. Salvador, J. J. Dannenberg, S. Dapprich, A. D. Daniels, Ö. Farkas, J. B. Foresman, J. V. Ortiz, J. Cioslowski and D. J. Fox, Gaussian, Inc., Wallingford CT, 2009.